Evaluation of Two-Layer Pavements Using Dimensional Analysis

LUTFI RAAD AND LYLA K. MARHAMO

Chart solutions for critical response parameters in two-layer pavements are developed using dimensional analysis. Multilayer elastic theory is applied, and simple dimensionless variables for critical response parameters are related to pavement geometry, material properties, and loading conditions. The solutions presented provide a comprehensive assessment of the physical behavior of two-layer systems under a wide variety of input variables. The proposed solutions are applied in the design and analysis of pavements using both functional and structural failure considerations.

Many transportation support systems could be modeled as two-layer structures. These structures could include, for example, a stabilized layer over subgrade or an existing pavement overlaid by a new surface layer. In general, pavements exhibit a wide range of material characteristics, such as complex particulate structure, stress-dependency, viscous and damping behavior, nonhomogeneity, and anisotropy. Although improved material models that simulate stress-dependent resilient behavior have been proposed and incorporate advanced numerical algorithms, such as the finite element method (*1,2*), the linear elastic theory is still considered by many to provide an acceptable approximation of real conditions. This theory, for example, is incorporated in a number of widely used design procedures, including those by Shell International Petroleum Company (*3*) and the Asphalt Institute (*4*). Moreover, a number of pavement evaluation methods that include nondestructive testing techniques use elastic theory to backcalculate average layer moduli that best fit surface deflection basins under applied loads (*5–7*). For pavement performance predictions, a number of limiting criteria have been expressed in terms of critical response parameters and number of load repetitions. These criteria are often determined from backcalculated stresses, strains, and deflections of existing field pavements using elastic theory (*8,9*). If such criteria are to be used in assessing pavement performance, the corresponding critical response parameters should be determined using similar analytical procedures, which will yield more meaningful and consistent predictions.

Dimensional analysis has been recognized by many investigators as a powerful tool for representing pavement analysis results (*10–13*). This method involves grouping analytical data into dimensionless parameters to provide an improved engineering approach for data presentation and interpretation. Chart solutions for critical response parameters in two-layer pavements are developed in the following paragraphs using dimensional analysis. Multilayer elastic theory is used, and simple dimensionless variables of critical pavement response parameters are related to pavement geometry, material properties, and loading conditions. The developed chart solutions, although complementary to other solutions and computer codes for predicting the response of pavement structures, have the added advantage of providing a simple and quick tool for the direct determination of critical response parameters in two-layer pavements. Moreover, they represent a comprehensive assessment of the physical behavior of two-layer pavements under a wide variety of input variables. The proposed solutions are applied here in the design and analysis of pavements using both functional and structural failure considerations.

L. Raad, Institute of Northern Engineering, University of Alaska, Fairbanks, Alaska 99775. L. K. Marhamo, Department of Civil Engineering, Massachusetts Institute of Technology, Cambridge, Mass. 02139.

ANALYSIS

Mechanistic methods of pavement design and evaluation require the determination of such critical response parameters as pavement stresses, strains, and deflections. In the two-layer systems analyzed, the response parameters include the following:

1. Tensile stresses and strains on the underside of the stabilized layer,
2. Vertical stresses and strains on top of the subgrade layer,
3. Surface deflections at the center of the applied load, and
4. Maximum shear stress in the subgrade.

These parameters are chosen on the basis of a number of pavement performance models (*3,8,9*). The two-layer system considered is shown in Figure 1.

Materials are assumed to be linear elastic, isotropic, and homogeneous. The surface layer is infinitely wide and has a uniform thickness H, a modulus of elasticity E_1, and Poisson's ratio ν_1. The subgrade layer is an elastic halfspace with elastic modulus E_2 and Poisson's ratio ν_2. The two-layer system is subjected to a uniform circular load having a radius R and intensity q. A summary of the cases analyzed is presented in Table 1. The following response parameters were determined using ELSYM5, a computer program for the analysis of elastic layers (*14*):

σ_x, ε_x = tensile stress and strain, respectively, on the underside of the stabilized layer;
σ_z, ε_z = vertical stress and strain, respectively, on top of the subgrade;

U = surface deflection at the center of the applied load; and

τ = maximum shear stress in the subgrade defined as $(\sigma_1 - \sigma_3)/2$, in which σ_1 and σ_3 are major and minor principal stresses, respectively.

These parameters were computed along the centerline of the applied surface load.

DIMENSIONLESS GROUPING OF RESPONSE PARAMETERS

Dimensional analysis was conducted to provide simple engineering solutions for pavement response parameters. These independent variables are grouped into (a) single-parameter correlations and (b) double-parameter correlations.

For single-parameter correlations, the required response parameters (i.e., stress, strain, and deflection) are expressed as follows:

$$X_i = f_i(E_1/E_2, H/R) \qquad i = 1 \text{ to } 6 \tag{1}$$

where X_i is a dimensionless parameter treated as an independent variable that could have the following forms:

$X_1 = \sigma_x/q$;

$X_2 = \sigma_z/q$;

$X_3 = \tau/q$;

$X_4 = E_2\varepsilon_x/q$;

$X_5 = E_2\varepsilon_z/q$; and

$X_6 = E_2U/Rq$.

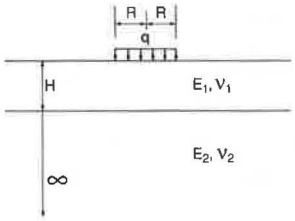

FIGURE 1 Representation of two-layer system.

Results of the analysis are shown in single-parameter charts (see Figures 2–7). These charts could be used to determine any of the response parameters defined in Equation 1. They also illustrate the trend of variation of these parameters in the practical ranges of E_1/E_2 and H/R.

Dimensional analysis was also conducted to develop double-parameter charts that would provide a more direct approach in the design and evaluation of two-layer pavements, particularly in relation to failure in the stabilized base or the subgrade. The dimensionless groupings are expressed as follows:

$$Y_i = g_i(Z_i, E_1/E_2, H/R) \qquad i = 1 \text{ to } 6$$

or

$$Z_i = W_i(Y_i, E_1/E_2, H/R) \qquad i = 1 \text{ to } 6 \tag{2}$$

where

$Y_1 = q/\sigma_z$;
$Y_2 = q/\sigma_z$;
$Y_3 = q/\tau$;
$Y_4 = q/\tau$;
$Y_5 = q/E_2\varepsilon_z$;
$Y_6 = q/E_2\varepsilon_z$;
$Z_1 = \sigma_x/\sigma_z$;
$Z_2 = E_2\varepsilon_x/\sigma_z$;
$Z_3 = \sigma_x/\tau$;
$Z_4 = E_2\varepsilon_x/\tau$;
$Z_5 = \sigma_x/E_2\varepsilon_z$; and
$Z_6 = \varepsilon_x/\varepsilon_z$.

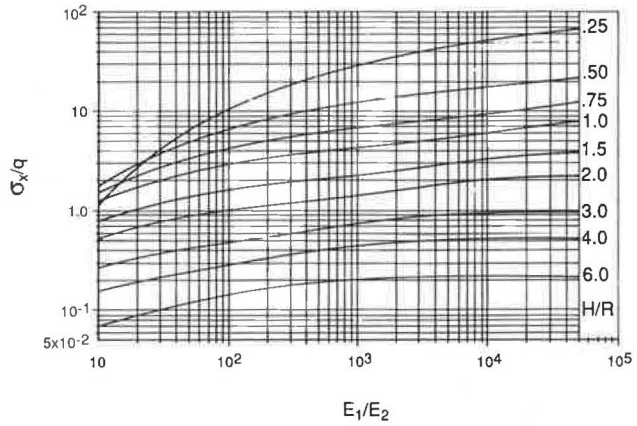

FIGURE 2 Solution chart for σ_x—two-layer theory.

TABLE 1 SUMMARY OF CASES ANALYZED

H/R	E_1/E_2	ν_1	ν_2
0.25, 0.50, 0.75, 1.0, 1.5, 2.0, 3.0, 4.0, 6.0	10,20,30,40,50,60,70,100,150, 200,300,400,500,600,700,1000, 1500, 2000,3000,4000,5000, 6000,7000,10000,15000 20000,30000,40000,5000	0.30	0.45

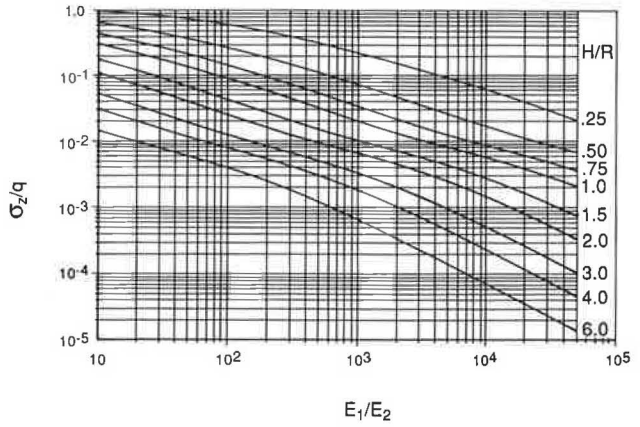

FIGURE 3 Solution chart for σ_z—two-layer theory.

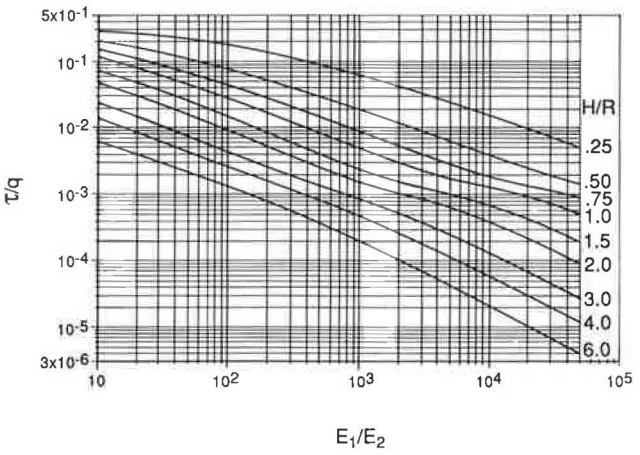

FIGURE 4 Solution chart for τ—two-layer theory.

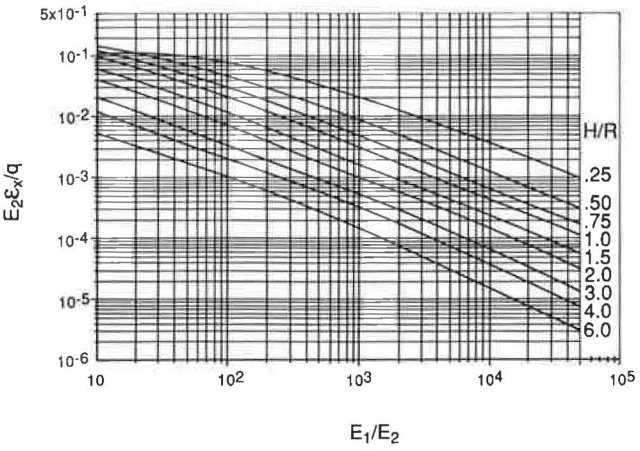

FIGURE 5 Solution chart for ε_x—two-layer theory.

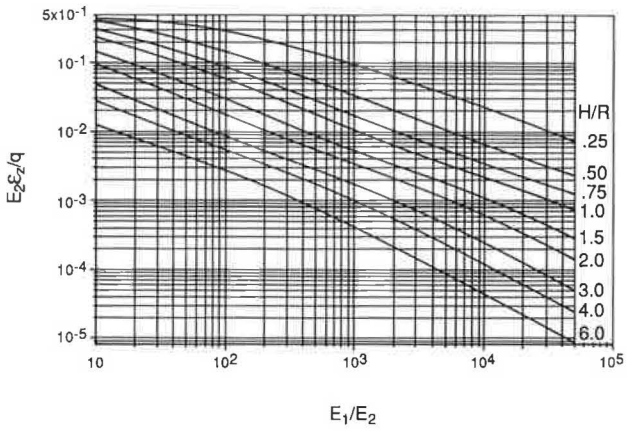

FIGURE 6 Solution chart for ε_z—two-layer theory.

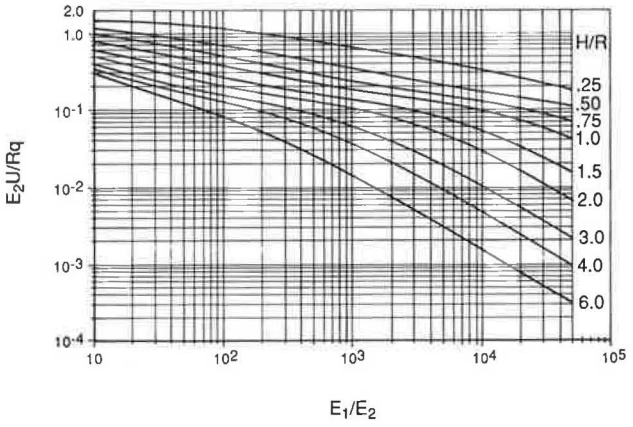

FIGURE 7 Solution chart for u—two-layer theory.

These correlations are presented in double-parameter charts, permitting the use of different combinations of pavement response variables in mechanistic design procedures (see Figures 8–13). In many cases, practical pavement design considerations require that fatigue failure of the stabilized base, rather than permanent deformation in the subgrade, be the governing performance criterion. This requirement necessitates the appropriate choice of pavement geometry (H/R) and material properties (E_1/E_2). In this regard, the ratio of response parameters defined by a given performance criteria (Z_i) should be less than the corresponding ratio resulting from the given loading condition.

APPLICATIONS

Results of dimensional analysis are used to assess the behavior of two-layer pavements under applied loads. Specifically, application of the proposed chart solutions in mechanistic pavement design and evaluation is illustrated using simple example problems. Furthermore, structural failure considerations are addressed, and improved solutions for predicting the structural capacity of two-layer systems are presented.

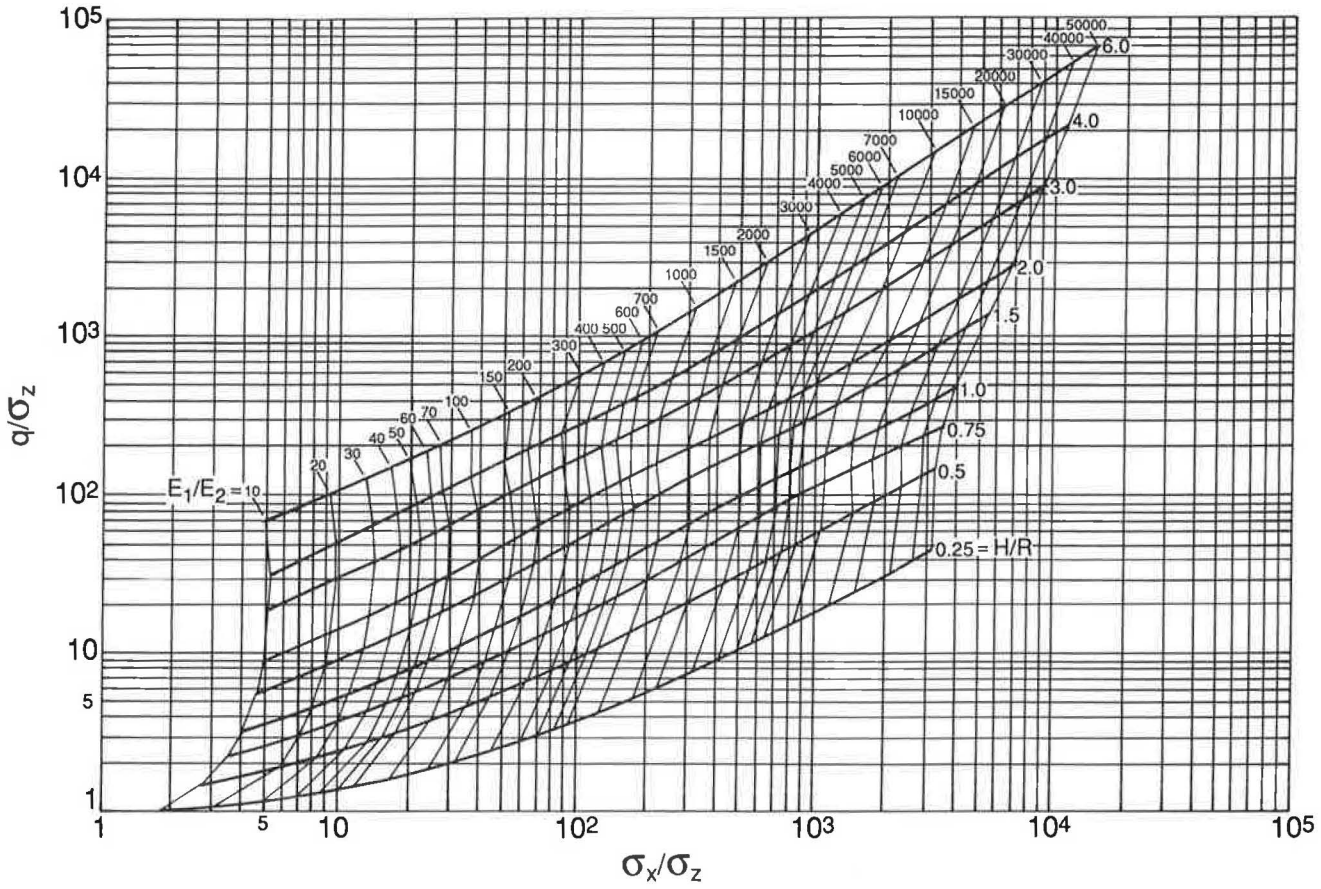

FIGURE 8 Solution chart for response parameters σ_x, σ_z—two-layer theory.

Mechanistic Pavement Design and Analysis

Example 1

Consider a pavement structure consisting of a stabilized base 15 in. thick having $E_1 = 200{,}000$ psi overlying a clay subgrade having $E_2 = 5{,}000$ psi. The pavement is subjected to a uniform tire pressure of 100 psi with a radius equal to 5 in. The tensile stress (σ_x) on the underside of the stabilized base and the vertical strain (ε_z) on top of the subgrade can be determined using Figure 12. In this case, $H/R = 3$ and $E_1/E_2 = 40$; therefore, $q/E_2\varepsilon_z = 58$ and $\sigma_x/E_2\varepsilon_z = 23$.

The corresponding values of ε_z and σ_x are

$$\varepsilon_z = \frac{100}{58 \times 5{,}000} = 3.45 \times 10^{-4}$$

$$\sigma_x = 23 \times 5{,}000 \times 3.45 \times 10^{-4} = 39.6 \text{ psi}$$

Example 2

If, in Example 1, it is required to determine the thickness of the stabilized base given the following limiting criteria: fatigue failure of stabilized base, $\sigma_x = 60$ psi, and permanent deformation failure of subgrade, $\varepsilon_z = 4 \times 10^{-4}$, then

$$q/E_2\varepsilon_z = \frac{100}{5{,}000 \times 4 \times 10^{-4}} = 50$$

From Figure 12, $E_1/E_2 = 40$, $H/R = 2.8$, and $\sigma_x/E_2\varepsilon_z = 22.4$; then $H = 2.8 \times 5 = 14$ in. and $\sigma_x = 5{,}000 \times 4 \times 10^{-4} \times 22.4 = 44.7$ psi.

The ratio $\sigma_x/E_2\varepsilon_z$ determined according to the given limiting criteria is

$$\sigma_x/E_2\varepsilon_z = \frac{60}{5{,}000 \times 4 \times 10^{-4}} = 30$$

For $E_1/E_2 = 40$ and H/R values ranging from 0.25 to 6, permanent deformation failure in the subgrade governs pavement performance provided $\sigma_x/E_2\varepsilon_z$, determined for a given set of limiting criteria, is greater than 23. In this example, $\sigma_x/E_2\varepsilon_z$ equals 30; hence, subgrade rutting precedes fatigue failure in the stabilized base. In order for fatigue to be the predominant mode of failure, pavement materials should conform to limiting criteria yielding values of $\sigma_x/E_2\varepsilon_z$ less than 14, as estimated from Figure 12 for $E_1/E_2 = 40$ and $H/R = 0.25$.

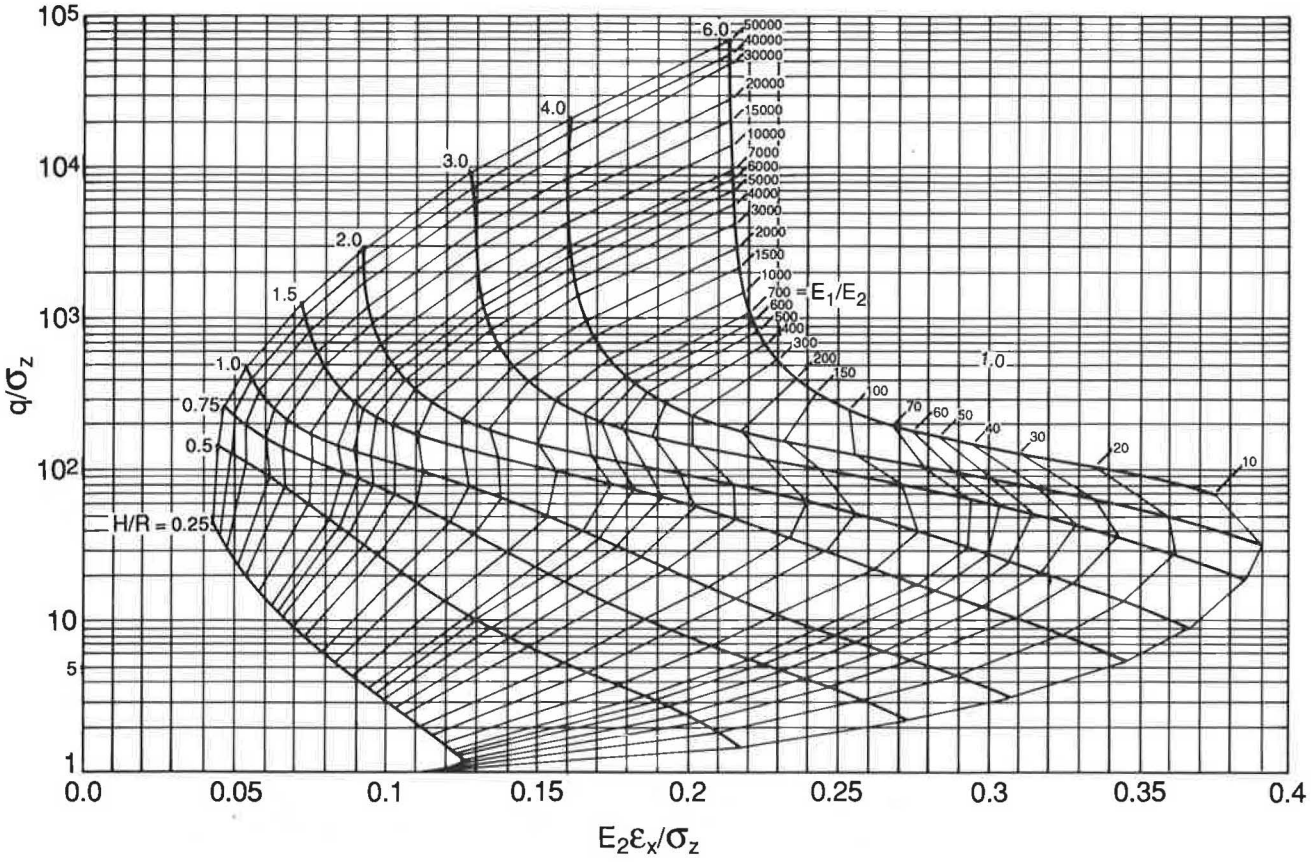

FIGURE 9 Solution chart for response parameters ε_x, σ_z—two-layer theory.

Structural Capacity Considerations

The overriding consideration in many pavement design problems is the serviceability and performance of the pavement structure under long-term repeated loading conditions. Mechanistic design procedures aim at minimizing fatigue and permanent deformation in the pavement system. In many cases, the structural adequacy of the pavement to support static loads or slowly moving loads needs to be addressed. Of particular significance in this case is the bearing capacity of the pavement structure. The bearing capacity of two-layer pavements consisting of a stabilized base over subgrade have been investigated by a number of researchers (*15–17*). The most comprehensive and complete work to date has been presented by Meyerhof (*15*), who used rigid-plastic analysis to determine the collapse load of concrete pavements. Meyerhof's work is applied here, together with results of dimensional analysis, to develop improved procedures of bearing capacity analysis.

The analysis assumes the following failure conditions:

1. Flexure failure initiation in the stabilized base,
2. Bearing capacity failure of the fine-grained subgrade, and
3. Ultimate collapse of the stabilized base.

Linear elastic analysis is used to address the first and second possible failure conditions. Flexure failure in the stabilized base occurs when the tensile stress (σ_x) on the underside of the base becomes equal to the flexure strength (T_f). Subgrade failure occurs when the vertical stress (σ_z) becomes equal to $6C$, where C is subgrade cohesion. This is consistent with bearing capacity estimates for saturated clays.

Flexure failure in the stabilized base and bearing capacity failure of the subgrade can be determined using the results of dimensional analysis presented previously. For example, chart solutions shown in Figure 8 can be used to determine the maximum and minimum ratios of σ_x/σ_z for a given E_1/E_2 and H/R ranging from 0.25 to 6. The maximum and minimum ratios of σ_x/σ_z are used to define the corresponding maximum and minimum values for the ratio of flexural strength of the stabilized base (T_f) to the cohesion of the subgrade (C) (i.e., $\sigma_x = T_f$, $\sigma_z = 6C$). This ratio is denoted as $(T_f/C)_l$, and its variation with E_1/E_2 is shown in Figure 14. For a given E_1/E_2, bearing capacity failure will initiate in the subgrade if the ratio T_f/C of the flexural strength of the stabilized layer to subgrade cohesion is greater than the maximum value of $(T_f/C)_l$. On the other hand, flexural failure initiation will occur if T_f/C is smaller than the minimum value of $(T_f/C)_l$. The ultimate surface pressure (q_u), associated either with bearing capacity failure of subgrade or with flexural failure of the base, is determined using the data in Figure 8. The variation of q_u with E_1/E_2 is shown in Figures 15 and 16. Estimates could be made for both interior and edge loading of base failure (Figure 15) and subgrade failure (Figure 16). Stresses

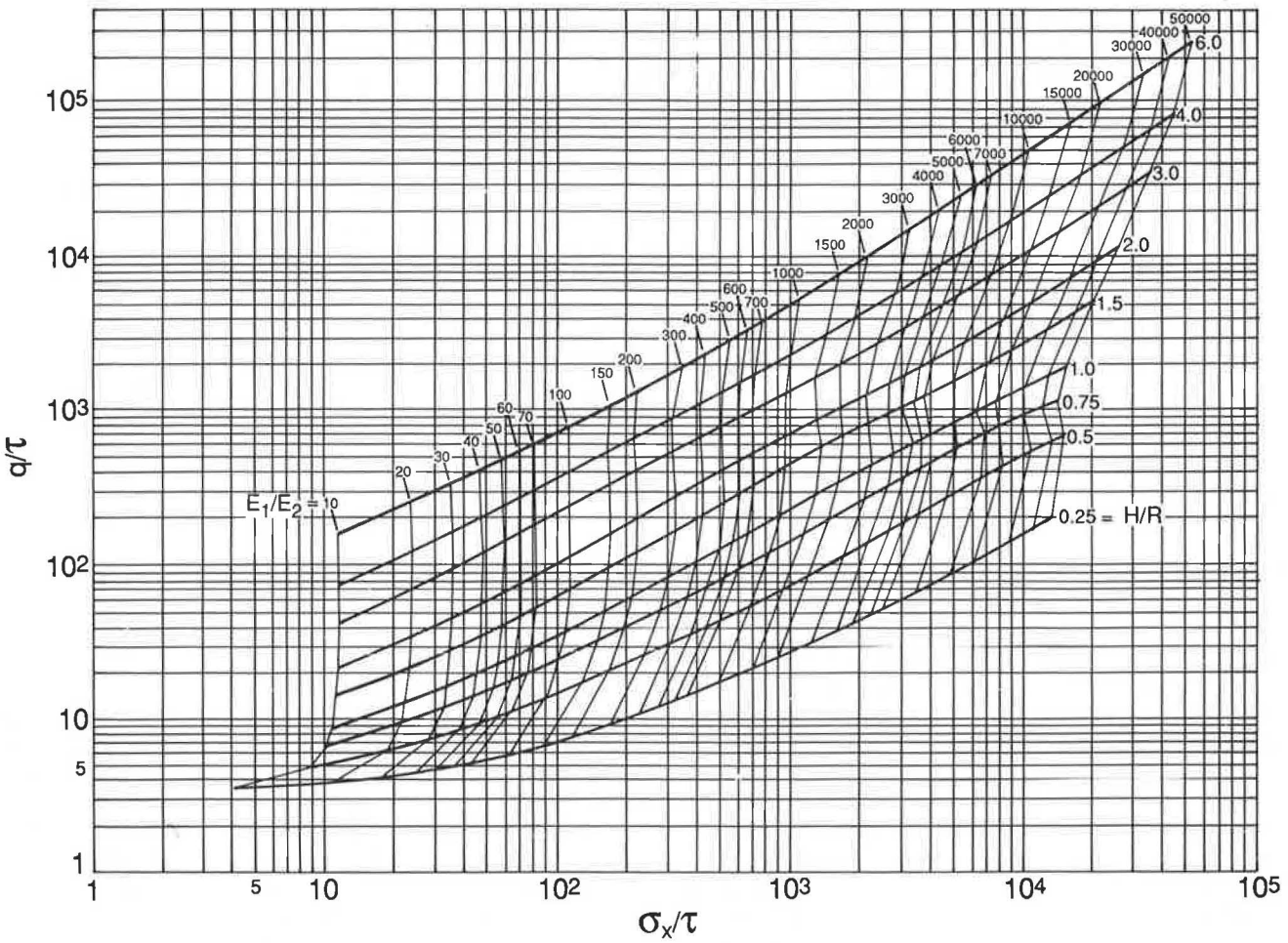

FIGURE 10 Solution chart for response parameters σ_x, τ—two-layer theory.

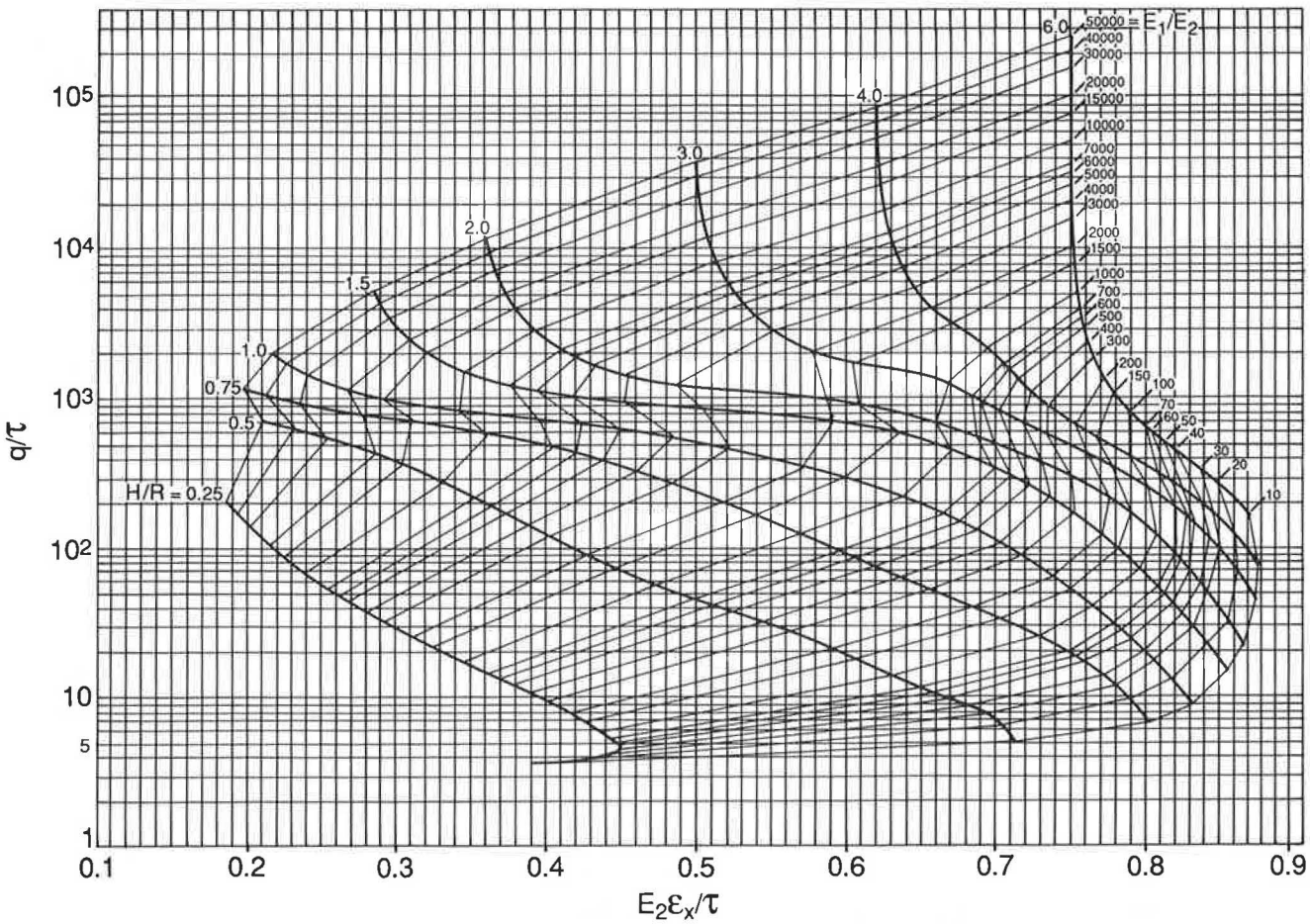

FIGURE 11 Solution chart for response parameters ε_x, τ—two-layer theory.

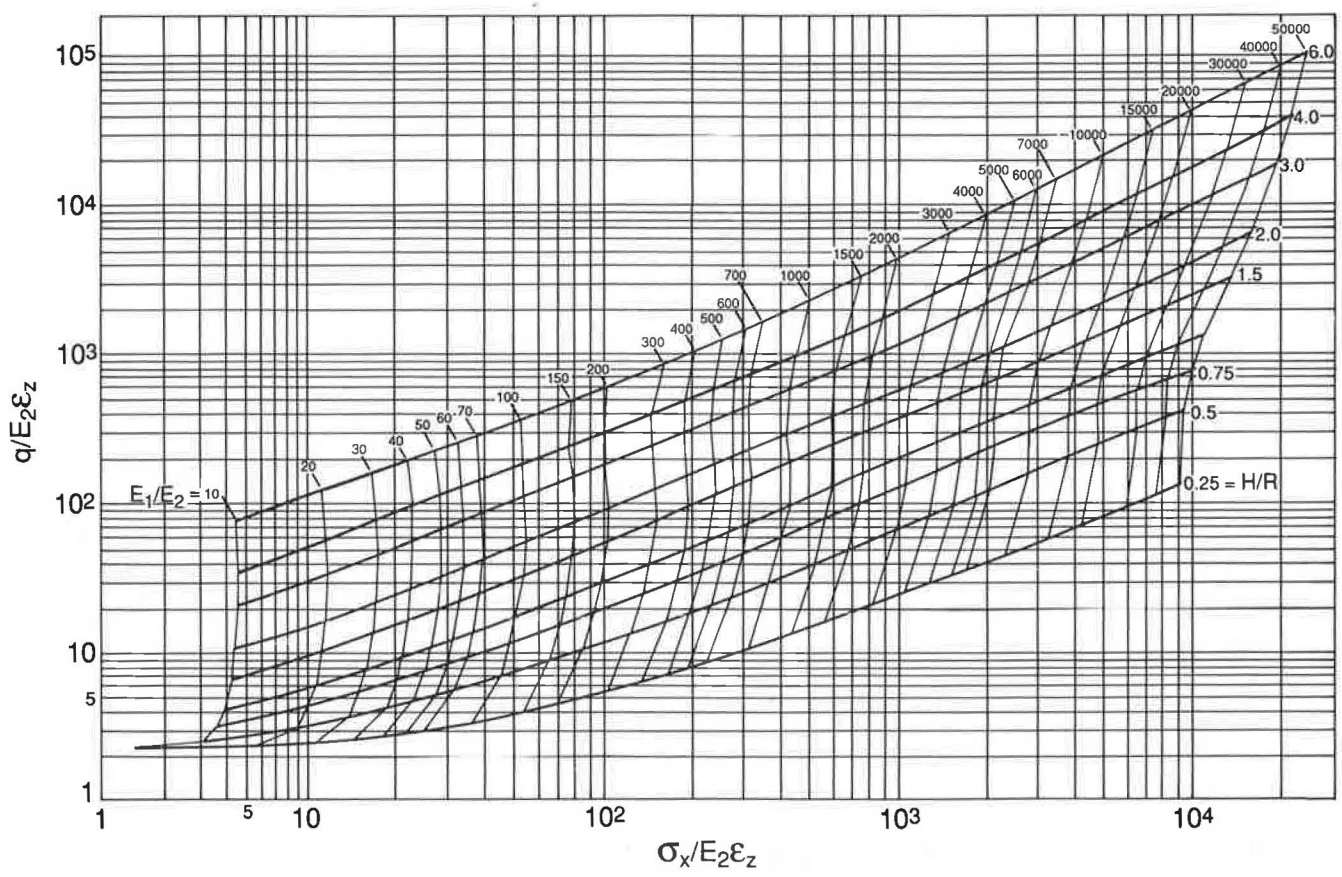

FIGURE 12 Solution chart for response parameters σ_x, ε_z—two-layer theory.

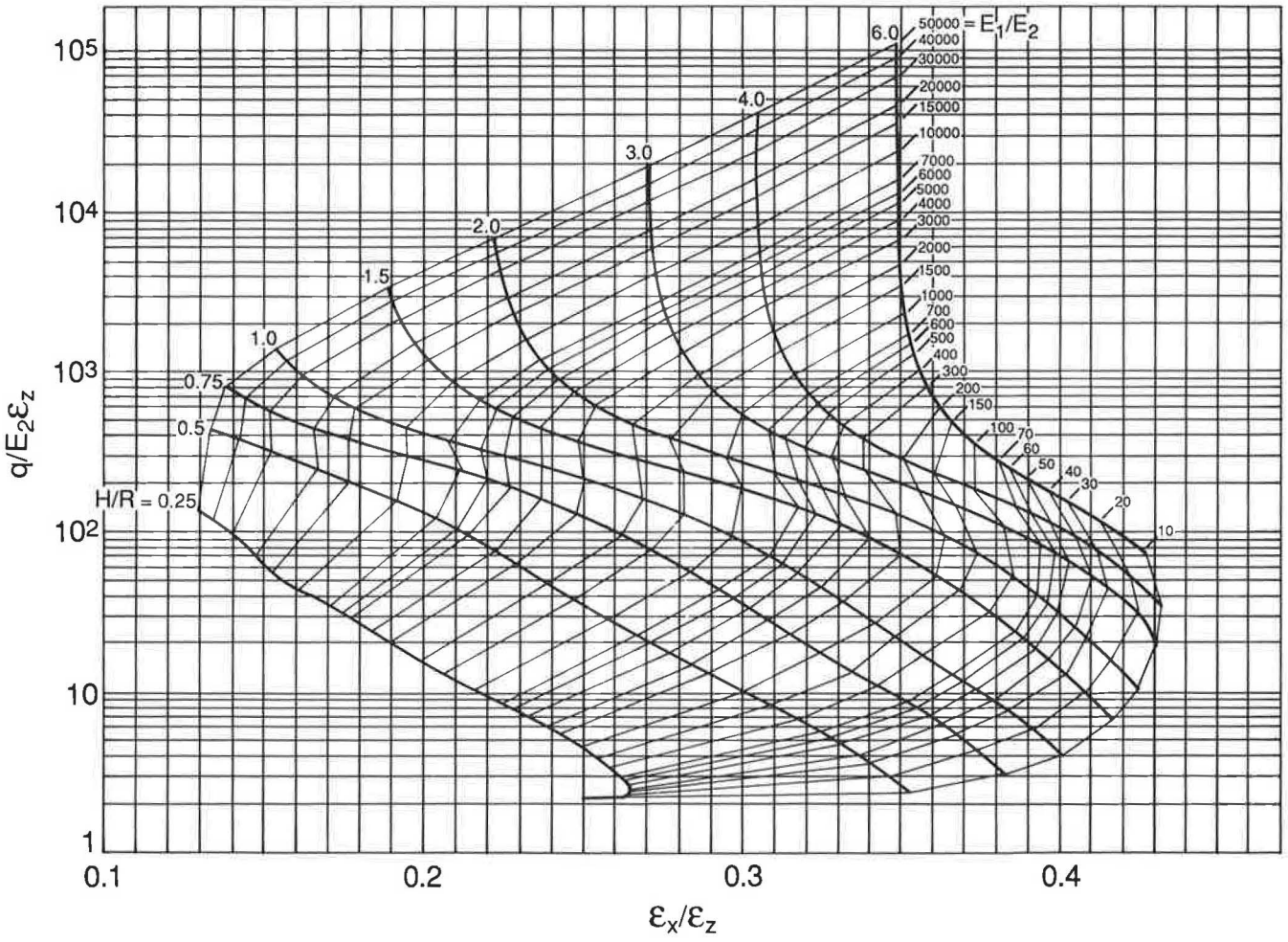

FIGURE 13 Solution chart for response parameters ε_x, ε_z—two-layer theory.

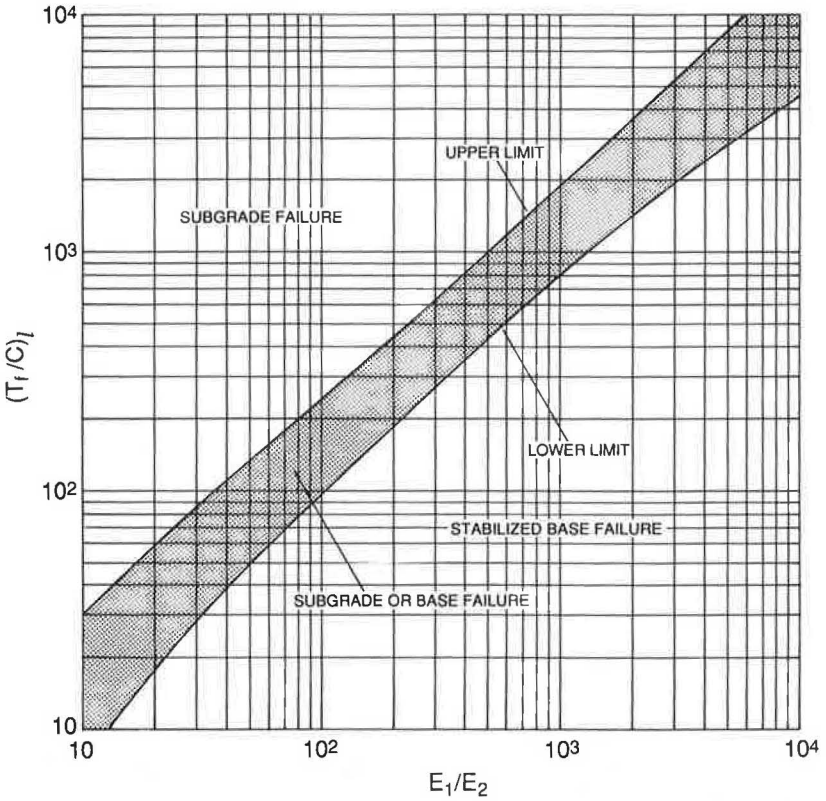

FIGURE 14 Limiting values for T_f/C associated with subgrade or base failure.

associated with edge loading are assumed to be 50 percent greater than those obtained for interior loading, as suggested by Mitchell et al. (*8*).

The ultimate collapse of the stabilized base follows flexural crack initiation on its underside or subgrade bearing capacity failure. The ultimate collapse load intensity (q_{uc}) is estimated using Meyerhof's approach (*15*). Meyerhof's equations could be rearranged and expressed as follows:

For interior loading,

$$\frac{q_{uc}}{T_f} = \frac{2/3}{(1 - R/3L)}\left(\frac{H}{R}\right)^2 \quad \left(\text{for } \frac{R}{L} > 0.2\right) \tag{3}$$

For edge loading,

$$\frac{q_{uc}}{T_f} = \left(\frac{\pi + 4}{6\pi}\right)\frac{1}{(1 - 2R/3L)}\left(\frac{H}{R}\right)^2 \left(\text{for } \frac{R}{L} > 0.2\right) \tag{4}$$

where L, the stiffness radius, is given by

$$L = \left[\frac{E_1(1 - \nu_2^2)H^3}{E_2(1 - \nu_1^2)^6}\right]^{1/3} \tag{5}$$

If failure initiation occurs in the stabilized base, the ultimate collapse load could be determined from Equation 3 or 4. In this case, it is assumed that, as cracking initiates on the underside of the base, both E_1 and E_2 will reduce and the ratio E_1/E_2 will remain essentially unchanged. Consequently, L will not change and q_{uc} will approach the same value predicted in Equations 3 and 4.

If, on the other hand, failure occurs first in the subgrade, then the subgrade modulus will decrease and approach zero and the corresponding value of R/L will also approach zero. For these conditions, a rigid-plastic behavior of the stabilized base will yield the following:

For interior loading,

$$\frac{q_{uc}}{T_f} = \frac{1}{3}\left(\frac{H}{R}\right)^2 \tag{6}$$

For edge loading,

$$\frac{q_{uc}}{T_f} = \left(\frac{\pi + 4}{12\pi}\right)\left(\frac{H}{R}\right)^2 \tag{7}$$

The collapse load, determined using rigid-plastic analysis, will correspond to the ultimate structural capacity of the system. A comparison between lower bound solutions for failure initiation q_u and ultimate collapse load intensity q_{uc} for the cases presented in Table 1 indicates that the ratio q_{uc}/q_u varies between 1 and 3.

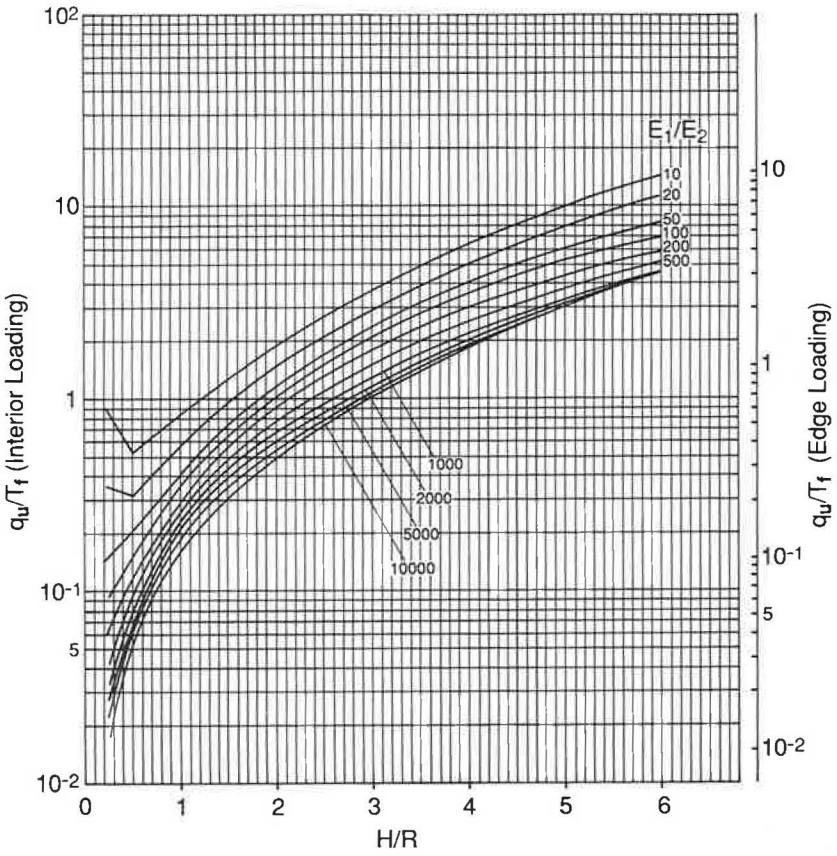

FIGURE 15 Surface load associated with flexure failure of base.

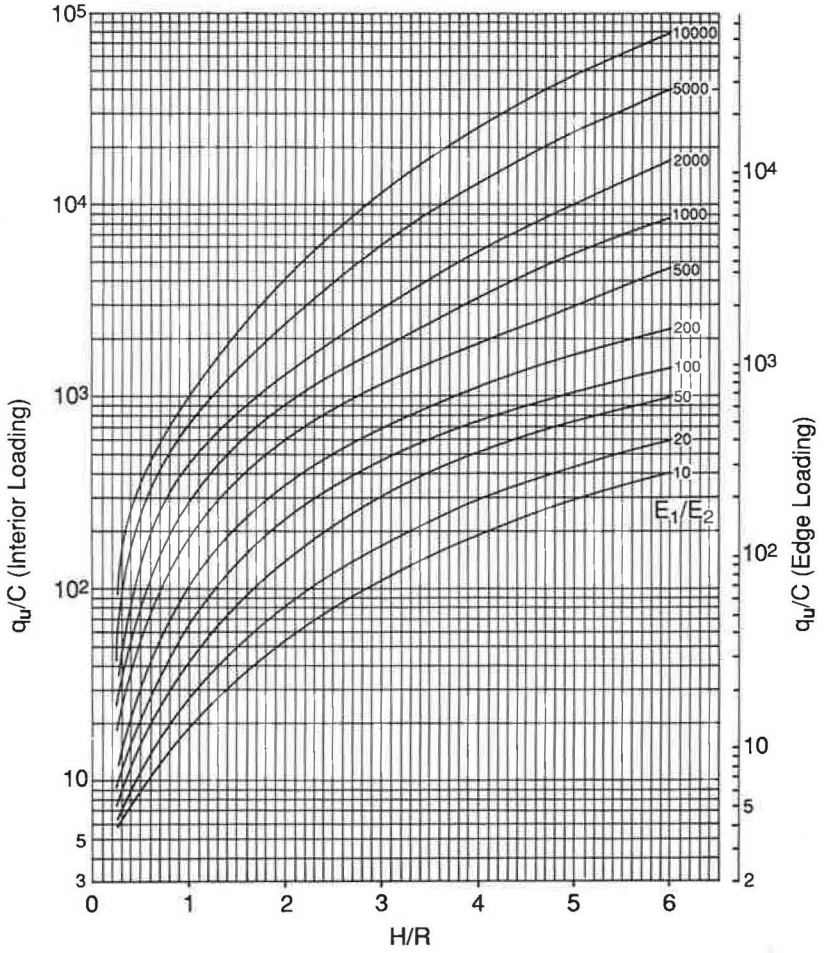

FIGURE 16 Surface load associated with bearing capacity failure of subgrade.

SUMMARY AND CONCLUSIONS

Dimensional analysis was applied to develop solutions for critical response parameters in two-layer pavements using linear elastic theory. Pavement response parameters, such as stresses, strains, and deflections, were grouped into dimensionless variables. Solutions were presented in charts that would allow simple determination of these parameters. These solutions could also be used to predict the performance of two-layer systems using available mechanistic models. Furthermore, these solutions could be implemented to assess whether fatigue failure in the surface layer or permanent deformation failure in the subgrade dominates the performance of the pavement under long-term repeated loads. Results of the analysis were also applied in developing an improved method to predict the structural capacity of stabilized layers over fine-grained subgrades under static or slowly moving loads.

The power of dimensional analysis in providing representative and simple engineering solutions for a wide range of pavement variables, including geometry, materials, and loading conditions, was illustrated. This capability is significant because of the need to develop meaningful interpretations of extensive experimental and analytical data as a result of ongoing pavement research programs.

REFERENCES

1. S. F. Brown and J. W. Pappin. Analysis of Pavements With Granular Basis. In *Transportation Research Record 810*, TRB, National Research Council, Washington, D.C., 1981, pp. 17–23.
2. L. Raad and J. L. Figueroa. Load Response of Transportation Support Systems. *Journal of the Transportation Engineering Division, ASCE*, Vol. 106, No. TE1, 1980, pp. 111–128.
3. *Shell Pavement Design Manual—Asphalt Pavements and Overlays for Road Traffic*. Shell International Petroleum Company Limited, London, England, 1978.
4. *Thickness Design—Asphalt Design for Air Carrier Airports*. Manual Series 11, 3rd ed., Asphalt Institute, College Park, Md., 1987.
5. R. L. Lytton. *Backcalculation of Pavement Layer Properties*. STP 1026. ASTM, Philadelphia, Pa., 1989, pp. 7–38.
6. L. H. Irwin. *User's Guide to MODCOMP2*. Cornell Local Roads Program Report 83-8. Cornell University, Ithaca, N.Y., 1983.
7. J. P. Mahoney, N. F. Coetzee, and R. N. Stubstad. *A Performance Comparison of Selected Backcalculation Computer Programs*. STP 1026. ASTM, Philadelphia, Pa., 1989, pp. 452–467.
8. M. I. Darter and A. J. Devos. *Structural Analysis of Asphaltic Cold Mixtures Used in Pavement Bases*. Research Report 505-4. Engineering Experiment Station, University of Illinois, Urbana, Aug. 1977.
9. M. W. Witczak. Design of Full Depth Asphalt Airfield Pavements. *Proc., 3rd International Conference on the Structural Design of Asphalt Pavements*, London, England, 1972, pp. 550–567.
10. D. M. Burmister. The Theory of Stresses and Displacements in Layered Systems and Application to the Design of Airport Runways. *HRB Proc.*, Vol. 23, 1943, pp. 126–144.
11. H. M. Westergaard. New Formulas for Stresses in Concrete Pavements of Airfields. *Transactions, ASCE*, Vol. 113, 1948, pp. 425–439.
12. K. R. Peattie. Stress and Strain Factors for Three Layer Elastic Systems. *Bulletin 342*, HRB, National Research Council, Washington, D.C., 1962.
13. A. M. Ioannides and R. A. Salsilli-Murua. Temperature Curling in Rigid Pavements: An Application of Dimensional Analysis. In *Transportation Research Record 1227*, TRB, National Research Council, Washington, D.C., 1989, pp. 1–11.
14. G. Ahlborn. *ELSYM5, A Computer Program for the Analysis of Elastic Layered Systems with Normal Loads*. ITTE, University of California, Berkeley, 1972.
15. G. G. Meyerhof. Load Carrying Capacity of Concrete Pavements. *Journal of the Soil Mechanics and Foundation Division, ASCE*, Vol. 88, No. SM3, June 1962, pp. 89–116.
16. L. Raad. Behavior of Stabilized Layers Under Repeated Loads. In *Transportation Research Record 1002*, TRB, National Research Council, Washington, D.C., 1985, pp. 72–79.
17. L. K. Marhamo. *Bearing Capacity of Cement-Treated Layers Over Soft Ground*. M.E. thesis. American University of Beirut.
18. J. K. Mitchell, P. Dzwilewski, and C. L. Monismith. *Behavior of Stabilized Soils Under Repeated Loading: A Summary Report with Suggested Structural Design Procedure*. Report 6. U.S. Army Engineer Waterways Experiment Station, Vicksburg, Miss., June 1974.

Publication of this paper sponsored by Committee on Flexible Pavement Design.